# Excited-State Dynamics of *trans*- and *cis*-Azobenzene after UV Excitation in the $\pi\pi^*$ Band

**H. Satzger, C. Root, and M. Braun***

*Sektion Physik, Ludwig-Maximilians-Universität, Oettingenstr. 67, D-80538 München, Germany*

*Received: February 3, 2004; In Final Form: April 30, 2004*

Transient absorption measurements on *cis*- and *trans*-azobenzene after UV excitation in the $\pi\pi^*$ band are presented and compared to data obtained after VIS excitation in the $n\pi^*$ band. The data show a two-step process, where after a fast motion on the $S_2$ potential energy surface the molecule relaxes to the $S_1$ state and in both cases (*trans* → *cis* and *cis* → *trans*) the isomerization reaction involves large-amplitude motion on the $S_1$ potential energy surface.

## 1. Introduction

Organic molecules that experience a large and reversible structural change after optical excitation are widely used as optical switches. Such optical switching molecules are for example implemented in the vision process (retinal chromophore in the visual protein rhodopsin) or photosynthesis in Archeae bacteria (retinal in bacteriorhodopsin). Another very prominent and technologically applied member of this family of molecules is azobenzene, which proved to be a candidate for the application as optical storage device.[1] In azobenzene, two benzene rings are connected via two double-bonded nitrogen atoms (azo group, N═N). Azobenzene has two isomers: the thermally stable *trans*-form and the metastable *cis*-form.[2] The large photoinduced structural change of this molecule was successfully used for example to control the helix content in a short peptide[3] and to optically trigger the folding reaction in a peptide ring.[4] In the *trans*-form the molecule is planar, whereas in the *cis*-form the benzene rings are clapped together. At room temperature the *cis*-form relaxes back thermally into the *trans*-form within several hours. In the electronic ground state the *cis*-state is higher in energy than the *trans*-state by 0.6 eV and reaches the *trans*-state only via a barrier of 1.6 eV.[2] The two configurations can be interchanged easily by optical excitation with light at suitable wavelengths. The isomerization process involves large-amplitude motion on the $S_1$ potential energy surface.

The absorption spectrum of azobenzene shows two distinct bands: a strong $\pi\pi^*$ absorption band peaking at ca. 290 nm (*cis*-form, depending on the solvent) and 320 nm (*trans*-form) and a much weaker $n\pi^*$ band with a peak around 440 nm (*cis*- and *trans*-form).

The *trans* → *cis* photoisomerization of azobenzene in solution occurs on the subpicosecond and picosecond time scale. After exciting the *trans*-isomer in the $n\pi^*$ band, the molecule leaves the Franck−Condon region and evolves on the $S_1$ potential energy surface. It reaches the transition region, presumably a conical intersection, where it interconverts to the ground-state potential energy surface and evolves to the *cis*-configuration with a quantum yield of ≈25%.[2] After excitation of the $\pi\pi^*$ transition, the isomerization reaction occurs with a different quantum yield of only 12%.[2] When the reaction starts from the *cis*-azobenzene, the *trans*-state is reached with a higher quantum yield of ≈50%.[2]

Several studies have dealt with the thermally stable *trans*-isomer in different solvents, with both $n\pi^*$ and $\pi\pi^*$ excitation.[5−10] Transient absorption experiments on *trans*-azobenzene in ethanol and DMSO for example showed biexponential kinetics of the isomerization process on the $S_1$ surface and internal conversion (0.32 and 2.1 ps in ethanol and 0.34 and 3.0 ps in DMSO[6,10]). Other experiments show similar kinetics with slightly changed time constants dependent on the solvent used.[5,7−9] Slower processes after internal conversion were assigned to the cooling dynamics of the hot molecules on the time scale between 5 and 20 ps.[11] The comparison of steady-state fluorescence and time-resolved transient absorption experiments allowed to distinguish different dynamics of processes of *trans*-azobenzene after $n\pi^*$ excitation: The observed absorption kinetics were assigned to the initial evolution of the molecule out of the Franck−Condon region (≈0.3 ps) and the second, diffusive motion on the $S_1$ potential energy surface toward the conical intersection (≈3 ps) where the internal conversion takes place.[10] Time-resolved fluorescence measurements[12] of the photoinduced *trans* → *cis* isomerization with a biexponential fluorescence decay (with decay times of 0.2 and 1 ps) support this interpretation.

In the *cis*-form the photoisomerization to the *trans*-form occurs ultrafast and with high quantum efficiency. Transient absorption experiments carried out on *cis*-azobenzene showed a faster process involving a dominating component with time constants of 0.17 ps in ethanol and 0.1 ps in DMSO and slower but much weaker components with time constants of ≈1 and ≈10 ps for both ethanol and DMSO.[6,10] This observation points to a steeper $S_1$ potential energy surface in the vicinity of the Franck−Condon region of *cis*-azobenzene, which is in accordance with theoretical calculations[13,14] and emission data.[10]

Many studies on the photoisomerization of azobenzene were performed after excitation of the lowest $n\pi^*$ transition of the molecule. For the excitation at higher energies via the $\pi\pi^*$ transition, several pathways have been proposed for the isomerization. Basically, one has the possibility of (i) an isomerization on the $S_2$ potential energy surface itself or (ii) a stepwise process with a fast internal conversion from the $S_2$ to the $S_1$ state followed by an isomerization on the $S_1$ potential energy surface. For the understanding of these processes, time-resolved experiments as well as the observed reduction of the isomerization

* Corresponding author: Fax +49-89/2180-9202; e-mail markus.braun@physik.uni-muenchen.de.

10.1021/jp049509x CCC: $27.50 
Published on Web 07/01/2004

quantum yield by a factor of 2 after $\pi\pi^*$ excitation (as compared to $n\pi^*$ excitation) have to be taken into account.

One step toward the understanding of processes originating from $\pi\pi^*$ excitation was undertaken by Schultz et al.[15] They have performed time-resolved photoelectron spectroscopy on *trans*-azobenzene in the gas phase after UV excitation with 330 nm. They concluded that by UV excitation several electronic states are populated: not only the $S_2$ state but also the $S_3$ and $S_4$ states. Approximately one-half of the population reaches the $S_2$ state and undergoes a fast transition to the $S_1$ state, from where it isomerizes. The population of the $S_3$ and $S_4$ states, having different symmetries compared to that of $S_2$, undergoes a direct, radiationless relaxation to the ground state. By this means, their model describes the observed factor of 2 in the isomerization quantum yield (0.12 for $\pi\pi^*$ excitation as compared to 0.25 for $n\pi^*$ excitation).

Fujino et al. have also performed transient absorption and time-resolved fluorescence spectroscopy on *trans*-azobenzene after 266 nm excitation.[16] They report $S_2 \rightarrow S_0$ as well as $S_1 \rightarrow S_0$ emission from azobenzene in hexane. Lifetimes for the $S_2$ state of 0.11 ps and for the $S_1$ state of 0.50 ps are reported. They explain the observed reduction in the isomerization quantum yield by the radiationless relaxation channel from a hot $S_1$ state to the ground state.

In this paper, we address photoisomerization of azobenzene after excitation of the $\pi\pi^*$ transition by femtosecond time-resolved absorption experiments. We present data for both the *trans* → *cis* and the *cis* → *trans* photoisomerization and compare the data with the different models proposed so far.

## 2. Experimental Section

Azobenzene was purchased from Merck (>98% purity, >97% *trans*) and used for the experiments without further purification. As a solvent, ethanol absolute from Merck was used. The concentration of azobenzene in ethanol was 2.2 mM, and a fresh sample was prepared for each experiment. To avoid changes in the isomer concentration by the femtosecond experiment, 50 mL of the sample was pumped through a quartz flow cell (optical path length of 0.5 mm). For the experiments on the *cis*-form, the sample was prepared by illumination of *trans*-azobenzene with a mercury lamp (1000 W Hg (Xe) lamp (Oriel), UG11 and WG305 (Schott, 2 mm) filters, 120 mW in the spectral region from 305 to 360 nm, exposure time 1 h). The progress of the photoreaction was monitored by absorption spectroscopy, and the illumination was stopped when the photostationary spectrum was reached. During the transient absorption experiment, the reservoir was continuously illuminated to keep the sample in the photostationary state. Absorption spectroscopy performed on the *cis*-sample after the experiment confirmed that the photostationary state was held throughout the experiment.

The laser setup consists of a homemade Ti:sapphire CPA (chirped pulse amplifier) system, which delivers 90 fs pulses at a central wavelength of 800 nm with a repetition rate of 1 kHz and a pulse energy of 1 mJ. A small part of the fundamental light was used to generate a UV−vis white-light continuum in a $CaF_2$ plate.[17] For the experiments with 266 nm excitation, 400 $\mu$J was used to generate 266 nm pulses by a two-step frequency tripling process: frequency doubling to 400 nm (in a BBO crystal, type I, 0.5 mm thick) and sum-frequency generation of 800 and 400 nm pulses in a BBO crystal (type I, 0.5 mm thickness). For the experiments with 340 nm excitation, a noncollinear optical parametric amplifier (NOPA)[18−20] was used to produce pulses at 680 nm, which were then frequency doubled to 340 nm in a thin BBO crystal (50 $\mu$m thickness). The cross-correlation width used for all transient absorption experiments was ca. 200 fs.

The sample was excited by the 266 nm (340 nm) pulse, and the transient absorption signal was measured with the UV−vis white light probe pulse spectrally resolved in a single shot detection setup consisting of a photodiode array, amplifier, and a 96-channel ADC device.[21] The sample was exchanged completely in the flow cell between two consecutive pump pulses.

In the thermal equilibrium at room temperature azobenzene is to 100% in its *trans*-form. After longtime illumination in the UV, a distinct amount of the molecules is brought to the *cis*-form (usually about 90%, depending on the solvent). Since both *cis*- and *trans*-azobenzene absorb in this spectral region, illumination is unable to produce 100% *cis*-samples. Only a photostationary equilibrium between *cis*- and *trans*-azobenzene with ≈90% *cis*-molecules is reached by illumination. By subtracting the absorption of the remaining *trans*-molecules, the absorption spectrum of the *cis*-isomer is obtained. By this procedure, we determined the remaining *trans*-form in the photostationary state to be ca. 12%. The transient absorption data were corrected for this amount of *trans*-molecules in the sample.

For every data point measured with a fixed delay time between pump and probe pulse, 10 000 single shots were averaged. The transient absorption of ethanol was subtracted from the sample signal, and the time traces at each wavelength were corrected for the corresponding chirp of the white-light continuum. To get a qualitative feeling for the number and the time scale of the involved kinetic processes, a data visualization technique based on the logarithmic differentiation of absorption changes (LDAC) was used.[22] In addition, by singular value decomposition, the number of involved kinetic components was also estimated. The thereby obtained information was used to derive starting values for a global least-squares fitting algorithm with sums of exponentials. Confidence intervals for the thereby obtained time constants have been estimated using an exhaustive search algorithm as reported in refs 22 and 23.

## 3. Experimental Results

***Trans* → *Cis* Photoreaction.** An overview of the time-resolved absorption data on *trans*-azobenzene in ethanol after $\pi\pi^*$ excitation with 266 nm pulses is presented in Figure 1a. The time axis is linear for delay times between −1 and 1 ps and logarithmic for longer delay times. Figure 2a shows transient spectra extracted from the data of Figure 1a at selected delay times. The transient absorption signal at 0.2 ps shows a pronounced maximum at 400 nm (80 nm fwhm) and an unstructured absorption signal over the whole observed spectral range (450−650 nm). This broad signal has completely vanished after 5 ps, whereas the peak at 400 nm decays slower and has vanished only after 20 ps. After 200 ps the stationary difference spectrum is reached. Figure 2b shows the transient spectra of *trans*-azobenzene after excitation with 340 nm pulses. There is a very close resemblance to the transients after 266 nm excitation. The only difference is seen in the transient taken after 0.2 ps, which shows slight modulations in the broad signal above 450 nm.

***Cis* → *Trans* Photoreaction.** The time-resolved absorption data on *cis*-azobenzene in ethanol after $\pi\pi^*$ excitation with 266 nm pulses are presented in Figure 1b as an overview. Figure 3 shows transient spectra extracted from the data of Figure 1b at selected delay times.

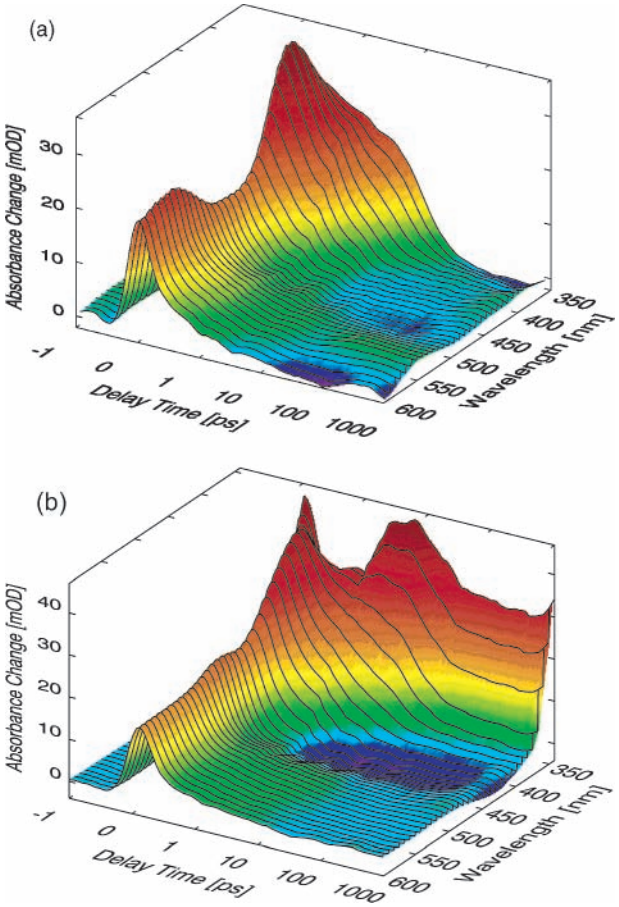


**Figure 1.** Transient absorption data of azobenzene in ethanol after 266 nm excitation: (a) *trans* → *cis*; (b) *cis* → *trans*.

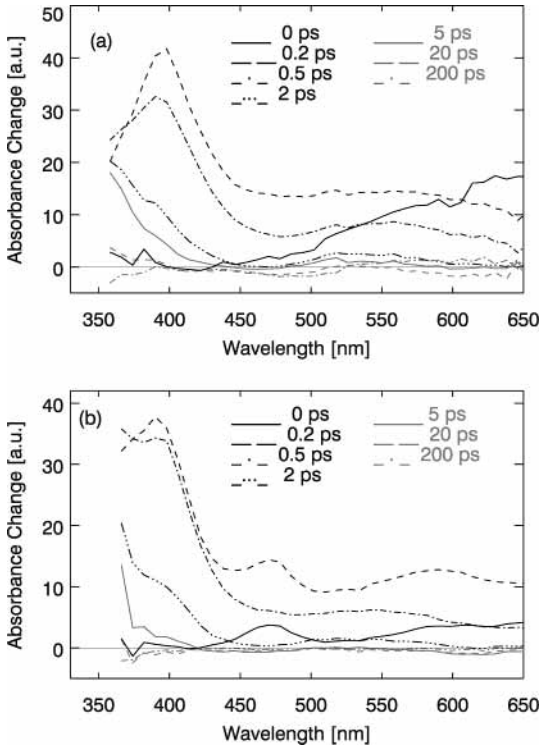


**Figure 2.** Transient spectra for azobenzene in ethanol after $\pi\pi^*$ excitation, *trans* → *cis* photoreaction: (a) 266 nm excitation, (b) 340 nm excitation.

The early transient spectrum taken after 0.2 ps shows a maximum centered at 380 nm (ca. 120 nm fwhm) and a broad, unstructured transient absorption above 450 nm. The behavior of the transient absorption is very similar to the *trans* → *cis* case: The maximum at 380 nm decays within several picoseconds, accompanied by a shift of the absorption maximum to the UV. The broad signal in the visible decays faster in a few picoseconds to a spectral shape that remains and only changes its amplitude until at 200 ps the stationary difference spectrum is reached.

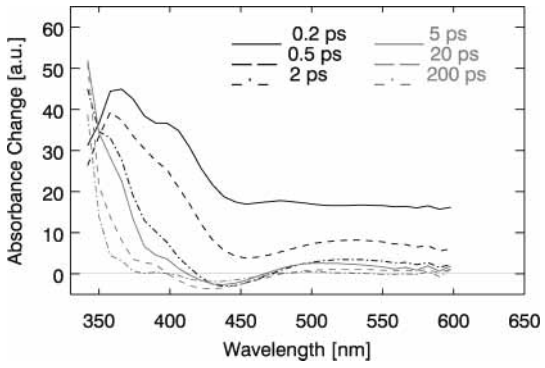


**Figure 3.** Azobenzene in ethanol, *cis* → *trans* after excitation with 266 nm pulses: transient spectra.

## 4. Modeling of the Data

***Trans* → *Cis* Photoreaction.** From earlier transient absorption studies after excitation of the n$\pi^*$ state it is known that the transient absorption data can be described using three exponential decay times of 0.34, 3.0, and 12 ps and an offset due to the metastable *cis*-photoproduct.[6,10] These values have therefore been taken as starting values for a global fitting routine to describe the transient absorption data after $\pi\pi^*$ excitation. The results from the global fitting algorithm showed that the experimental data require an additional short time constant of $\approx$0.1 ps in order to explain the observed absorption spectra (this was confirmed by SVD and LDAC methods). Considering time-zero and cross-correlation width of pump and probe pulse, the data are described best by the sum of four exponentials and a long-lasting absorption change. The determined time constants are $0.13^{0.09}_{0.17}$, $0.42^{0.33}_{0.50}$, $2.9^{1.9}_{4.4}$, and $12^{8.8}_{15}$ ps (the subscript and superscript values are upper and lower error estimates which have been computed using an exhaustive search algorithm as reported in refs 22 and 23). The decay associated spectra for the four time constants are shown in Figure 4a (266 nm excitation). The modeling of the data measured with 340 nm excitation yielded time constants of $0.13^{0.11}_{0.19}$, $0.43^{0.30}_{0.76}$, $2.7^{2.5}_{2.8}$, and $17^{5}_{32}$ ps (amplitude spectra shown in Figure 4b). Considering the confidence intervals for each time constant, the decay times for 266 and 340 nm excitation are identical. Therefore, only one set of time constants (0.13, 0.42, 2.9, and 12 ps) will be used further on to describe both experiments. Comparing the values of the three slower time constants and considering the confidence intervals, it is obvious that the decay times of 0.42, 2.9, and 12 ps match perfectly the ones obtained after n$\pi^*$ excitation.[10] In addition, their respective decay associated spectra match well the spectra obtained from n$\pi^*$ excitation (see Figure 5a and ref 10). As a consequence, these three processes seem to be very similar for $\pi\pi^*$ and n$\pi^*$ excitation. Nevertheless, there are distinct differences in the dynamics observed after exciting *trans*-azobenzene in the $\pi\pi^*$ band.

(i) Most noticeable is a new time constant of 0.13 ps, not seen before in the transient absorption after n$\pi^*$ excitation of *trans*-azobenzene (see Figure 5a). The decay associated spectrum of this component shows minima at 400 and 530 nm, which

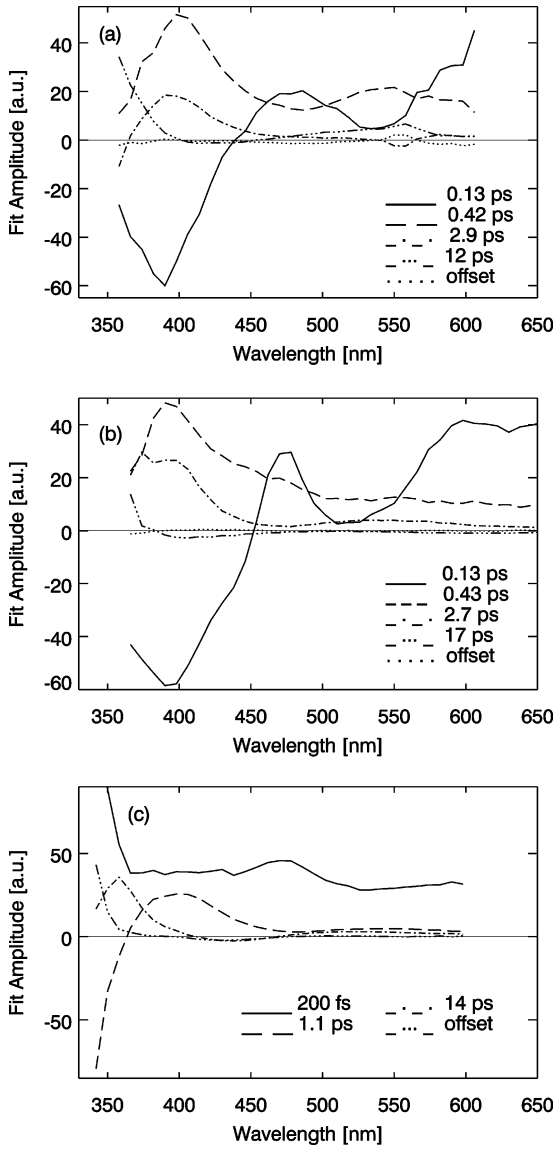


**Figure 4.** Decay associated spectra for azobenzene in ethanol: (a) 266 nm excitation (*trans* → *cis*), (b) 340 nm excitation (*trans* → *cis*), (c) 266 nm excitation (*cis* → *trans*).

may be due to the buildup of transient absorption (the decay of this absorption is found to occur with time constants of 0.42 and 2.9 ps). As can be seen from Figure 2a,b, the initial transient spectrum at 0 ps delay time consists of an excited-state absorption above 450 nm, and the excited-state absorption feature at 400 nm (seen in the 0.2 ps transient spectrum) shows a delayed rise, indicating a sequential process.

(ii) A broad transient absorption signal with peaks at 470 and 600 nm is found. It appears instantaneously with the excitation pulse.

(iii) The relative intensities of the decay associated spectra for 0.42 and 2.9 ps are different. Even though the spectral shapes of the two signals are similar, the transient absorption amplitude of the state connected to the 0.42 ps decay time is strongly enhanced after $\pi\pi^*$ excitation.

(iv) After $\pi\pi^*$ excitation, there is an enhancement and slight broadening of the sinusoidal transient absorption signal below 370 nm with a rise time of 0.42 and 2.9 ps and a decay with 12 ps. A sinusoidal shape in a transient absorption spectrum points to a time-dependent broadening of a spectral band.

***Cis* → *Trans* Photoreaction.** The decay times obtained from n$\pi^*$ excitation have been used as starting values for a global fitting algorithm (0.1, 1, and 10 ps). In contrast to the results for *trans*-azobenzene, no additional time constant is needed to describe the data on *cis*-azobenzene for $\pi\pi^*$ excitation. The obtained decay times are $0.200^{0.167}_{0.226}$, $1.1^{0.89}_{1.3}$, and $14^{11}_{17}$ ps and an offset. The decay associated spectra are shown in Figure 4c. As for the *trans* → *cis* isomerization data, the dynamics initiated by n$\pi^*$ and $\pi\pi^*$ excitation are very similar (see Figure 5b). However, there are two major differences: (i) The initial fast component of 0.17 ps (n$\pi^*$ excitation) is slowed down to 0.2 ps ($\pi\pi^*$ excitation). (ii) The intensities and spectral shape of the decay associated spectra for the two slower time constants are different. The intensities of the sinusoidal spectra are higher, and the bands are noticeably broader. This increase and broadening is observed best for the dominant $\pi\pi^*$ absorption band at short wavelengths.

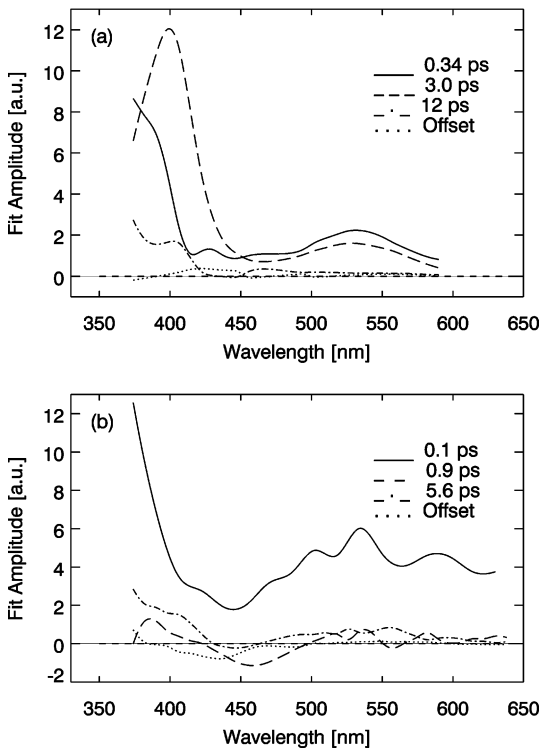


**Figure 5.** Decay associated spectra for azobenzene in DMSO after n$\pi^*$ excitation: (a) *trans* → *cis*, (b) *cis* → *trans* (the data are taken from ref 10).

This difference is quite reasonable as a very different electronic state is populated by the excitation pulse. Nevertheless, it should be noticed that the spectral shapes and associated decay times for the subsequent processes are very similar to the n$\pi^*$ excitation.

## 5. Interpretation on a Molecular Level

***Trans* → *Cis* Photoreaction.** For the *trans* → *cis* isomerization reaction after $\pi\pi^*$ excitation (at 266 or 340 nm), four time constants are needed to describe the observed dynamics. The three slower times of 0.42, 2.9, and 12 ps and their respective spectral shape are well-known from transient absorption studies after excitation of the n$\pi^*$ state (0.34, 3.0, and 12 ps). As these three decay times and the associated spectral shapes are not changed much upon $\pi\pi^*$ excitation, the interpretation of the molecular dynamics connected to the three transients is adopted. This means that the time constants of 0.42 and 2.9 ps belong to the movement out of the Franck−Condon region and internal conversion to the *cis*-ground state (0.42 ps) and an intermediate state on the $S_1$ potential energy surface that

isomerizes slower (2.9 ps, see also refs 6 and 10). The slowest time constant of 12 ps with its sinusoidal spectral shape is associated with cooling of the hot ground state due to the surrounding solvent.[11] Nevertheless, there are several changes in the dynamics observed after exciting the *trans*-form of the azobenzene molecule in the $\pi\pi^*$ band. As mentioned above, a short time constant of 0.13 ps was necessary to describe the data. This component has a decay associated spectrum that shows negative bands at 390 and 510 nm (see Figure 4a,b). Since the $S_1$ transient absorption spectrum peaks at these wavelengths, the 0.13 ps component can be explained as a buildup of a population of the $S_1$ state. Furthermore, this is justified as this transient absorption is absent in the initial transient absorption spectrum at 0 ps (see Figure 2a,b). With the same time constant of 0.13 ps, we observe the decay of a transient absorption signal (maximum at 470 and 600 nm). It appeared instantaneously with the pump pulse and therefore is interpreted as transient absorption from the directly populated $S_2$ state, in good agreement with results from Fujino et al.[8,16] As the further time constants and spectral shapes remain similar, it is reasonable to assign the 0.13 ps time constant to the radiationless relaxation process from the $S_2$ state to the $S_1$ potential energy surface. Subsequently, the isomerization takes place with similar dynamics as after n$\pi^*$ excitation. When comparing the transient absorption signals of the 0.42 and 2.9 ps components, a second difference between n$\pi^*$ and $\pi\pi^*$ excitation becomes obvious. These two time constants are connected to transient absorption of the Franck−Condon state (reached after $S_0 \rightarrow S_1$ n$\pi^*$ excitation) and intermediate states on the $S_1$ potential energy surface. Even though the overall spectral shapes of the two signals are similar, the transient absorption amplitude of the Franck−Condon state (0.42 ps) is strongly enhanced after $\pi\pi^*$ excitation. This leads to the interpretation that the excited molecule reaches the $S_1$ potential energy surface in a different geometry than the $S_0 \rightarrow S_1$ Franck−Condon region and that therefore the branching ratio of the fast (0.42 ps) and slow (2.9 ps) component is changed. It could be argued that identical isomerization processes after n$\pi^*$ and $\pi\pi^*$ excitation would call for absolutely identical decay associated spectra and time constants for the 0.42 and 2.9 ps processes. However, trying to describe both data sets (n$\pi^*$ and $\pi\pi^*$ excitation data) with identical time constants and decay associated spectra would introduce constraints into the fitting procedure. The data sets presented here have been fitted with amplitudes and time constants as completely free floating parameters. As this constraint-free procedure gives very similar time constants and also very similar decay associated spectra, we see this as evidence for the proposed identical isomerization pathways with a changed branching ratio on the $S_1$ potential energy surface.

As already mentioned, the further relaxation pathway including the cooling process is unchanged. We conclude that also the same intermediate state is populated and the $S_1$ potential energy surface is reached on a different point, but near the Franck−Condon region. A third difference in the $\pi\pi^*$ excitation data as compared to the n$\pi^*$ excitation is seen in the ground-state cooling signal, which manifests itself as a sinusoidal signal in the transient absorption below 370 nm. (A sinusoidal shape in a transient absorption spectrum appears when the internal temperature of the molecule leads to a time-dependent broadening of a spectral band.) The signal rises with a time constant of 0.42 and 2.9 ps and shows a decay rate of 12 ps. After $\pi\pi^*$ excitation, this signal is now enhanced and broadened, which can be explained by the higher excess energy of the UV pump pulse photons as compared to the visible excitation.

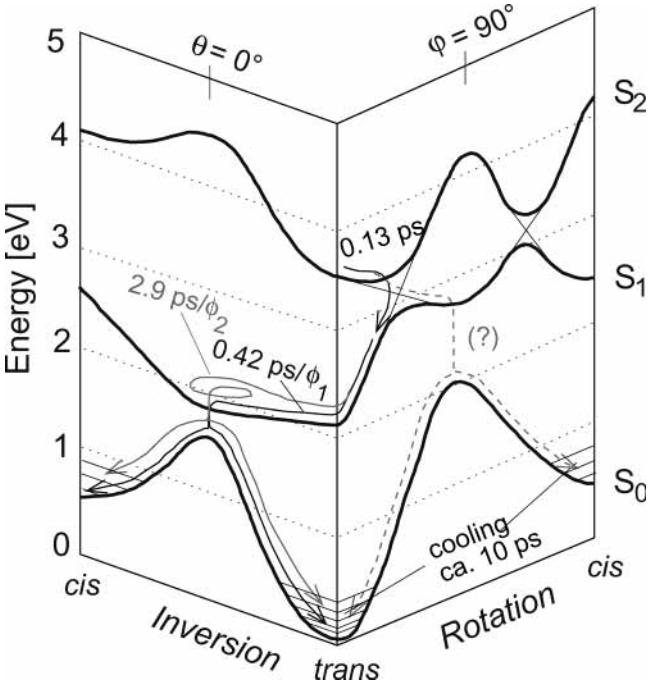


**Figure 6.** Scheme of the *trans* → *cis* isomerization process after $\pi\pi^*$ excitation based on calculations reported in ref 13 (see also ref 7). The $S_2$ state is populated and makes a fast movement along the rotational coordinate toward the $S_1$ potential energy surface with a time constant of 0.13 ps, which is reached with high excess energy. As can be seen from the slope of the $S_1$ surface, the further isomerization reaction then proceeds via the inversion coordinate to the *cis*-ground state. Here, a branching takes place, where a larger part of the molecules make a direct movement to the conical intersection (0.42 ps, isomerization quantum yield $\phi_1$) and fewer molecules follow a diffusive path (2.9 ps, isomerization quantum yield $\phi_2$, indicated by the loop). The potential energy landscape shows also the possibility of a branching at the transition point between $S_2$ and $S_1$ potential energy surface with a further isomerization along the rotational coordinate. The question mark indicates that the spectroscopic data do not support that such a way is taken.

This interpretation is visualized in the scheme of Figure 6, which is drawn according to Monti et al.:[13] After excitation in the $\pi\pi^*$ absorption band, the $S_2$ state is populated and makes a fast movement along the rotational coordinate toward the $S_1$ potential energy surface (0.13 ps), which is reached with high excess energy. As can be seen from the slope of the $S_1$ surface, the further isomerization reaction then proceeds via the inversion coordinate to the *cis*-ground state. Because the $S_1$ potential energy surface is reached with higher excess energy, a larger part of the molecules make a direct movement to the conical intersection (0.42 ps) and fewer molecules follow a diffusive path (2.9 ps).

The potential energy landscape shows also the possibility of a branching at the transition point between $S_2$ and $S_1$ potential energy surface with a further isomerization along the rotational coordinate. However, the spectroscopic data do not indicate that such a way is taken.

As pointed out by Schultz et al., the states $S_3$ and $S_4$ are nearly isoenergetic to $S_2$[15] (see also ref 14). It is therefore possible that by $\pi\pi^*$ excitation a population of these states is generated which makes a direct movement along the rotational coordinate back to the *trans*-ground state and therefore would reduce the overall isomerization quantum yield.

***Cis* → *Trans* Photoreaction.** In contrast to the *trans* → *cis* photoisomerization, the differences between n$\pi^*$ and $\pi\pi^*$

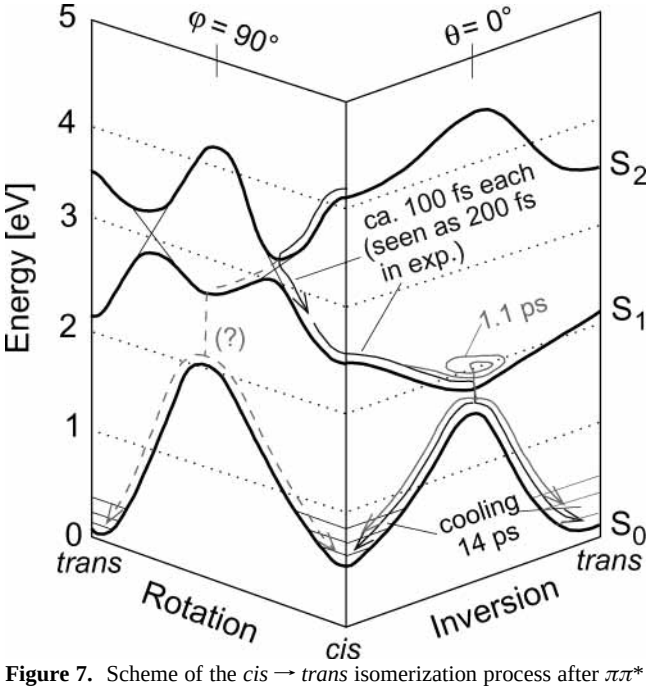


**Figure 7.** Scheme of the *cis* → *trans* isomerization process after $\pi\pi^*$ excitation based on calculations reported in ref 13. The $S_2$ state is populated and makes a fast movement along the rotational coordinate toward the $S_1$ potential energy surface, which is reached with high excess energy. The experimental data suggest a sequential dynamics $S_2 \rightarrow S_1$ and $S_1 \rightarrow S_0$ with time constants of about 0.1 ps each, not distinguishable in the experiment and described with only one time constant of 0.2 ps. On the $S_1$ potential energy surface, a small part of the molecules take a diffusive pathway toward the *trans*-ground state (time constant of 1.1 ps, indicated by the loop). Here, the intermolecular cooling process takes place with 14 ps. As in Figure 6, the potential energy landscape shows also the possibility of a branching at the transition point between $S_2$ and $S_1$ potential energy surface along the rotational isomerization coordinate. The question mark indicates that the spectroscopic data do not support that such a way is taken.

excitation are more subtle for the *cis* → *trans* reaction. Again, as for the data on *trans*-azobenzene, the dynamics initiated by $n\pi^*$ and $\pi\pi^*$ excitation are very similar. In the case of $n\pi^*$ excitation a fast component of 0.17 ps (azobenzene in ethanol, 0.1 ps for azobenzene in DMSO) describes the direct *cis* → *trans* isomerization process on a steep $S_1$ excited-state potential energy surface (movement out of the Franck−Condon region and isomerization process). A part of the molecules make a diffusive movement on the $S_1$ potential energy surface before it reaches the *trans*-ground state (2 ps in ethanol, 0.9 ps in DMSO).[6] Finally, the molecule transfers the heat to the solvent with a time constant of ca. 10 ps.[6,10] As mentioned above, the $\pi\pi^*$ excitation data are described best also with the sum of three exponentials plus an offset. The decay times and decay associated spectra are very similar. Thus, the interpretation of the decay processes after $n\pi^*$ excitation is adopted also for the processes following $\pi\pi^*$ excitation. The initial isomerization takes places with 0.2 ps, the diffusive movement is connected to the 1.1 ps time constant, and the intermolecular cooling is measured to occur with a 14 ps time constant. The shapes of the three signals are very similar to the respective spectra after $n\pi^*$ excitation (see Figures 4c and 5b). However, two differences have to be discussed. The direct isomerization process shows a noticeably longer decay time, although more excess energy is available. This slowdown can be explained if a similar two-step process as for the *trans* → *cis* isomerization after $\pi\pi^*$ excitation is assumed. In this case, an initial relaxation from the $S_2$ to the $S_1$ potential energy surface in about 0.13 ps precedes the 0.17 ps isomerization process. These two processes could not be resolved as the time constants are close together. The second difference is related to the cooling dynamics of the system as the intensities of the sinusoidal spectra are higher and the bands are obviously broader than after $n\pi^*$ excitation, even though the thermalization times are not noticeably changed ($n\pi^*$ excitation: 10 ps;[6] $\pi\pi^*$ excitation: 14 ps). This indicates that after $\pi\pi^*$ excitation in the UV a higher excess energy of the pump photon leads to a hotter molecule in the ground state. As predicted by the theoretical work of Cattaneo and Persico,[14] an ultrafast isomerization is found after $\pi\pi^*$ excitation.

As above, this interpretation is visualized in the scheme of Figure 7: After excitation in the $\pi\pi^*$ absorption band, the $S_2$ state is populated and makes a fast movement along the rotational coordinate toward the $S_1$ potential energy surface (0.13 ps), which is reached with high excess energy. The fast time constant is somehow slowed down to 0.2 ps because these two fast processes $S_2 \rightarrow S_1$ and $S_1 \rightarrow S_0$ are described with only one time constant. A small part of the molecules take a diffusive pathway toward the *trans*-ground state. Here, the intermolecular cooling process takes place with 14 ps.

As in Figure 6, the potential energy landscape shows also the possibility of a branching at the transition point between $S_2$ and $S_1$ potential energy surface along the rotational isomerization coordinate. As above, the spectroscopic data do not indicate that such a way is taken.

Our spectroscopic findings will now be discussed with regard to different isomerization models. Three models for the azobenzene relaxation after $\pi\pi^*$ excitation are discussed in the literature: (1) a two-step process, where in the first step the $S_2$ state relaxes to the $S_1$ state and there the isomerization process takes place;[5,7−9,16] (2) a direct isomerization on the $S_2$ potential energy surface;[2,24] (3) mixed population: after UV excitation, not only the $S_2$ state but also the $S_3$ and $S_4$ states are populated.[15]

*To Model 1*: Fujino et al. have also performed transient absorption and time-resolved fluorescence spectroscopy on *trans*-azobenzene in hexane after 266 nm excitation, extracting lifetimes for the $S_2$ state of 0.11 ps and for the $S_1$ state of 0.50 ps.[16] They explain the observed reduction in the isomerization quantum yield by the radiationless relaxation channel from a hot $S_1$ state to the ground state (rotational deactivation).

The data presented here support model 1 insofar as all observed time constants for *trans* → *cis* and *cis* → *trans* isomerization are very similar, and the intermediate state on the $S_1$ potential energy surface is observed. The additional 0.13 ps time can be explained as relaxation to the $S_1$ potential energy surface. Especially in the *trans* → *cis* data the unchanged time constants and spectra for the 0.42 and 2.9 ps processes assigned to the isomerization movement of the azobenzene molecule itself suggest that the isomerization takes place on the same energy surface as for $n\pi^*$ excitation. According to Fujino et al., the reduction of the isomerization quantum yield after $\pi\pi^*$ excitation has its origin in an additional radiationless relaxation pathway back to the *trans*-state due to a hot molecule on the $S_1$ potential energy surface (rotational deactivation). In addition to this radiationless channel, one has to consider a changed branching ratio on the $S_1$ potential energy surface. By this process, the reduction of the overall isomerization quantum yield from 25 ($n\pi^*$ excitation) to 12% ($\pi\pi^*$ excitation) could be explained.

*To Model 2*: A completely different isomerization pathway on the $S_2$ potential energy surface would imply different intermediate states and therefore different decay associated spectra. As can be seen in Figures 4 and 5, the decay associated

spectra after n$\pi$* and $\pi\pi$* excitation look very similar, and therefore, no indication of an alternative isomerization pathway could be found.

*To Model 3*: Similar as in model 1, the very isomerization involves large-amplitude motion on the $S_1$ potential energy surface after a fast radiationless relaxation $S_2 \rightarrow S_1$. The difference in isomerization quantum yield is now explained by incorporating the electronic states $S_3$ and $S_4$. As already mentioned, the $\pi\pi$* excitation pulse also generates population in these states. The movement out of the $S_2$ state in the gas phase was measured by Schultz et al. with 0.17 ps and the movement out of the $S_{3,4}$ state with 0.42 ps. As can be seen in Figure 4a,b, the decay associated spectra of the 0.13 ps component show the decay of the broad $S_2 \rightarrow S_N$ transient absorption signal, overlaid with an absorption recovery that peaks at 390 and 510 nm. This recovery is seen only for the fastest time constant in our experiment (0.13 ps). This seems to support a branching of the pathways from the $S_2$ state, where one part of the molecules undergo a transition to the $S_1$ potential energy surface (from where it isomerizes) and the other part moves directly along the rotational coordinate back to the *trans*-ground state. The time constants obtained by photoelectron spectroscopy for the relaxation of the $S_{3,4}$ state and by transient absorption spectroscopy for the direct isomerization pathway on the $S_1$ potential energy surface are exactly the same (0.42 ps). Our experiment is therefore not able to decide whether the $S_{3,4}$ state is substantially populated, but the decay associated spectra connected to the 0.42 ps component can be consistently explained simply by the well-known $S_1$ state dynamics. Since the $\pi\pi$* excitation has been performed by 266 and 340 nm in our experiment, one could expect different populations of the $S_2$ and $S_{3,4}$ states and therefore different dynamics. However, the observed decay associated spectra and decay times are very similar for both excitation wavelengths.

Models 1 and 3 agree on the statement that the isomerization involves large-amplitude motion on the $S_1$ potential energy surface. Extending model 1, one should consider that the two observed possible pathways on the $S_1$ potential energy surface (0.42 and 2.9 ps—both leading to the isomerization of the molecule) are connected to different isomerization quantum yields. Therefore, the measured change in relative amplitude of the transient absorption connected to these processes should be considered as an explanation for the change in the isomerization quantum yield. In this picture, no new relaxation pathways have to be introduced into the model.

## 6. Conclusion

In this paper, transient absorption data of *trans*-azobenzene and of *cis*-azobenzene after $\pi\pi$* excitation have been presented and compared to $n\pi$* excitation data. The experimental results indicate that in both cases (*trans* → *cis*) and (*cis* → *trans*) the isomerization reaction can be described by a two-step process, where after a short relaxation on the $S_2$ potential energy surface (decay time 0.13 ps) the main isomerization motion takes place on the $S_1$ potential energy surface. The difference as compared to n$\pi$* excitation is that the isomerization reaction starts on a different point on the $S_1$ potential energy surface (outside the Franck−Condon region). This causes different relative intensities of the decay associated spectra. Nevertheless, the spectral shapes and decay times of the spectral components are similar to the ones obtained after n$\pi$* excitation.

**Acknowledgment.** The authors thank W. Zinth, J. Wachtveitl, and P. Gilch for many discussions. This work was supported by the Deutsche Forschungsgemeinschaft (SFB 533).

## References and Notes

(1) Ikeda, T.; Tsutsumi, O. Optical Switching and Image Storage by Means of Azobenzene Liquid-Crystal Films. *Science* **1995**, *268*, 1873−1875.

(2) Rau, H. Azo compounds. In Dürr, H., Bouas-Laurent, H., Eds.; *Studies in Organic Chemistry, Photochroism, Molecules and Systems*; Elsevier-Verlag: Amsterdam, 1990; Vol. 40, Chapter 4, pp 165−192.

(3) Flint, D. G.; Kumita, J. R.; Smart, O. S.; Woolley, G. A. Using an Azobenzene Cross-Linker to Either Increase of Decrease Peptide Helix Content upon Trans-to-Cis Photoisomerization. *Chem. Biol.* **2002**, *9*, 391−397.

(4) Spörlein, S.; Carstens, H.; Satzger, H.; Renner, C.; Behrendt, R.; Moroder, L.; Tavan, P.; Zinth, W.; Wachtveitl, J. Ultrafast spectroscopy reveals subnanosecond peptide conformational dynamics and validates molecular dynamics simulation. *Proc. Natl. Acad. Sci. U.S.A.* **2002**, *99*, 7998−8002.

(5) Lednev, I. K.; Ye, T.; Hester, R. E.; Moore, J. N. Femtosecond Time-Resolved UV−Visible Absorption Spectroscopy of *trans*-Azobenzene in Solution. *J. Phys. Chem.* **1996**, *100*, 13338−13341.

(6) Nägele, T.; Hoche, R.; Zinth, W.; Wachtveitl, J. Femtosecond photoisomerization of cis-azobenzene. *Chem. Phys. Lett.* **1997**, *272*, 489−495.

(7) Lednev, I. K.; Ye, T.; Matousek, P.; Towrie, M.; Foggi, P.; Neuwahl, F. V. R.; Umapathy, S.; Hester, R. E.; Moore, J. N. Femtosecond time-resolved UV−Visible absorption spectroscopy of trans-azobenzene: dependence on excitation wavelength. *Chem. Phys. Lett.* **1998**, *290*, 68−74.

(8) Fujino, T.; Tahara, T. Picosecond Time-Resolved Raman Study of *trans*-Azobenzene. *J. Phys. Chem. A* **2000**, *104*, 4203−4210.

(9) Fujino, T.; Arzhansev, S. Yu.; Tahara, T. Femtosecond Time-Resolved Fluorescence Study of Photoisomerization of *trans*-Azobenzene. *J. Phys. Chem. A* **2001**, *105*, 8123−8129.

(10) Satzger, H.; Spörlein, S.; Root, C.; Wachtveitl, J.; Zinth, W.; Gilch, P. Fluorescence Spectra of trans- and cis-azobenzene—Emission from the Franck−Condon state. *Chem. Phys. Lett.* **2003**, *372*, 216−223.

(11) Hamm, P.; Ohline, S. M.; Zinth, W. Vibrational cooling after ultrafast photoisomerization of azobenzene by femtosecond infrared spectroscopy. *J. Chem. Phys.* **1997**, *106*, 519−529.

(12) Lu, Y.-C.; Chang, C. W.; Diau, E. W.-G. Femtosecond fluorescence dynamics of *trans*-azobenzene in hexane on excitation to the $S_1(n,\pi^*)$ state. *J. Chin. Chem. Soc. Taip.* **2002**, *49*, 693−701.

(13) Monti, S.; Orlandi, G.; Palmieri, P. Features of the photochemically active state surfaces of azobenzene. *Chem. Phys.* **1982**, *71*, 87−99.

(14) Cattaneo, P.; Persico, M. An ab initio study of the photochemistry of azobenzene. *Phys. Chem. Chem. Phys.* **1999**, *1*, 4739−4739.

(15) Schultz, Th.; Quenneville, J.; Levine, B.; Toniole, A.; Martinez, T. J.; Lochbrunner, S.; Schmitt, M.; Shaffer, J. P.; Zgierski, M. Z.; Stolow, A. Mechanism and Dynamics of Azobenzene Photoisomerization. *J. Am. Chem. Soc.* **2003**, *125*, 8098−8099.

(16) Fujino, T.; Arzhansev, S. Yu.; Tahara, T. Femtosecond/Picosecond Time-Resolved Spectroscopy of *trans*-Azobenzene: Isomerization Mechanism Following $S_2(\pi\pi^*) \rightarrow S_0$ Photoexcitation. *Bull. Chem. Soc. Jpn.* **2002**, *75*, 1031−1040.

(17) Huber, R.; Satzger, H.; Zinth, W.; Wachtveitl, J. Noncollinear optical parametric amplifiers with output parameters improved by the application of a white light continuum generated in $CaF_2$. *Opt. Commun.* **2001**, *194*, 443−448.

(18) Wilhelm, T.; Piel, J.; Riedle, E. Sub-20-fs pulses tunable across the visible from a blue-pumped single-pass noncollinear parametric converter. *Opt. Lett.* **1997**, *22*, 1494−1497.

(19) Lochbrunner, S.; Wilhelm, T.; Piel, J.; Spörlein, S.; Riedle, E. Sub-20-fs tunable pulses in the visible and NIR by noncollinear optical parametric amplification (NOPA). In Fejer, M. M., Injeyan, H., Keller, U., Eds.; *OSA Trends in Optics and Photonics*; OSA: Washington, DC, 1999; Vol. 26, p 366.

(20) Riedle, E.; Beutter, M.; Piel, J.; Schenkl, S.; Spörlein, S.; Zinth, W. Generation of 10 to 50 fs pulses tunable through all of the visible and the NIR. *Appl. Phys. B: Laser Opt.* **2000**, *71*, 457−465.

(21) Seel, M.; Wildermuth, E.; Zinth, W. A multichannel detection system for application in ultrafast spectroscopy. *Meas. Sci. Technol.* **1997**, *8*, 449−452.

(22) Satzger, H.; Zinth, W. Visualization of transient absorption dynamics—towards a qualitative view of complex reaction kinetics. *Chem. Phys.* **2003**, *295*, 287−295.

(23) Roelofs, T. A.; Lee, C.-H.; Holzwarth, A. R. Global target analysis of picosecond chlorophyll fluorescence kinetics from pea chloroplasts. *Biophys. J.* **1992**, *61*, 1147−1163.

(24) Rau, H. Further evidence for rotation in the $\pi,\pi^*$ and inversion in the $n,\pi^*$ photoisomerization of azobenzenes. *J. Photochem.* **1984**, *26*, 221−225.